exhibited the same initial response to such injections, namely, intense scratching of the injection sites, all of the MC-deficient $Kit^{W\text{-}sh}/Kit^{W\text{-}sh}$ mice, but none of the wild-type mice or the wild-type BMCMC-engrafted $Kit^{W\text{-}sh}/Kit^{W\text{-}sh}$ mice, developed gross hematuria (Fig. 4).

Although the extent to which MCs might be able to enhance resistance to other animal venoms remains to be determined, components of the venoms of many different animals can activate MCs (*7*) (SOM Text 3). Moreover, it is quite possible that MC mediators, in addition to CPA and other proteases, also may contribute to the ability of MCs to reduce the morbidity and mortality associated with certain venoms. In 1965, Higginbotham hypothesized that MCs can reduce the toxicity of Russell's viper venom by degranulating and releasing heparin, which then binds highly cationic components of the venom and thereby reduces its toxicity (*27*). However, this interesting hypothesis has not yet been tested using MC-deficient and MC-engrafted mice (SOM Text 4). Finally, it is of course possible that MCs might contribute to (or have no effect on) the toxicity observed with some venoms.

We have identified a heretofore unproven role for MCs: enhancing innate host resistance to the toxicity of certain animal venoms. Our observations also provide a new perspective on the presence, within MCs, of prominent cytoplasmic granules that contain a large amount and, in some species, a large diversity, of proteases (*28*, *29*). It is likely that mast cell proteases can have beneficial roles in many settings, not only in host defense (*23*, *28*, *30*). However, we speculate that the storage in MC cytoplasmic granules of large amounts of proteases, which can be released to the exterior very rapidly upon suitable MC activation, reflects, at least in part, the selective pressure of the exposure of animals to diverse exogenous toxins (such as those in vertebrate and invertebrate venoms and perhaps those produced by certain microorganisms), as well as the advantage of being able to degrade and thereby control the toxicity of potent endogenous molecules such as ET-1 (*16*) (SOM Text 5).

References and Notes

1. B. G. Fry *et al.*, *Nature* **439**, 584 (2006).
2. J. P. Chippaux, *Bull. World Health Organ.* **76**, 515 (1998).
3. R. D. Theakston, D. A. Warrell, E. Griffiths, *Toxicon* **41**, 541 (2003).
4. A. Rucavado, T. Escalante, J. M. Gutierrez, *Toxicon* **43**, 417 (2004).
5. J. White, *Toxicon* **45**, 951 (2005).
6. N. K. Dutta, K. G. Narayanan, *Nature* **169**, 1064 (1952).
7. A. Weisel-Eichler, F. Libersat, *J. Comp. Physiol. A Neuroethol. Sens. Neural Behav. Physiol.* **190**, 683 (2004).
8. D. D. Metcalfe, D. Baram, Y. A. Mekori, *Physiol. Rev.* **77**, 1033 (1997).
9. M. F. Gurish, K. F. Austen, *J. Exp. Med.* **194**, F1 (2001).
10. H. Turner, J. P. Kinet, *Nature* **402**, B24 (1999).
11. F. D. Finkelman, M. E. Rothenberg, E. B. Brandt, S. C. Morris, R. T. Strait, *J. Allergy Clin. Immunol.* **115**, 449 (2005).
12. B. Echtenacher, D. N. Männel, L. Hültner, *Nature* **381**, 75 (1996).
13. R. Malaviya, T. Ikeda, E. Ross, S. N. Abraham, *Nature* **381**, 77 (1996).
14. A. P. Prodeus, X. Zhou, M. Maurer, S. J. Galli, M. C. Carroll, *Nature* **390**, 172 (1997).
15. M. Maurer *et al.*, *J. Exp. Med.* **188**, 2343 (1998).
16. M. Maurer *et al.*, *Nature* **432**, 512 (2004).
17. Y. Kloog *et al.*, *Science* **242**, 268 (1988).
18. Materials and methods are available as supporting material on *Science* Online.
19. E. Kochva, *Public Health Rev.* **26**, 209 (1998).
20. T. Nakano *et al.*, *J. Exp. Med.* **162**, 1025 (1985).
21. M. Tsai *et al.*, *Proc. Natl. Acad. Sci. U.S.A.* **97**, 9186 (2000).
22. K. P. Metsärinne *et al.*, *Arterioscler. Thromb. Vasc. Biol.* **22**, 268 (2002).
23. E. Tchougounova, G. Pejler, M. Abrink, *J. Exp. Med.* **198**, 423 (2003).
24. D. McNamee, *Lancet* **357**, 1680 (2001).
25. M. R. Ziai, S. Russek, H. C. Wang, B. Beer, A. J. Blume, *J. Pharm. Pharmacol.* **42**, 457 (1990).
26. M. C. Calixto, K. M. Triches, J. B. Calixto, *Inflamm. Res.* **52**, 132 (2003).
27. R. D. Higginbotham, *J. Immunol.* **95**, 867 (1965).
28. C. Huang, A. Sali, R. L. Stevens, *J. Clin. Immunol.* **18**, 169 (1998).
29. G. H. Caughey, *Mol. Immunol.* **38**, 1353 (2002).
30. J. Mallen-St. Clair, C. T. Pham, S. A. Villalta, G. H. Caughey, P. J. Wolters, *J. Clin. Invest.* **113**, 628 (2004).
31. J. O. Schmidt, *Toxicon* **33**, 917 (1995).

32. We thank E. Kochva and A. Bdolah for providing *Atractaspis engaddensis* venom and for helpful discussions, D. E. Clouthier and M. M. Yanagisawa for providing $ET_A^{-/-}$ and $ET_A^{+/-}$ ES cells, R. L. Stevens and R. Adachi for calling our attention to the similarities between vertebrate mast cells and ascidian test cells, and M. Liebersbach and A. Xu for technical assistance. This work was supported by NIH grants R37 AI23990, R01 CA72074, and P50 HL67674 (to S.J.G.) and by grants from the Deutsche Forschungsgemeinschaft (ME2668/1-1 to M.M.) and the Boehringer Ingelheim Fonds (to V.L.).

Supporting Online Material

www.sciencemag.org/cgi/content/full/313/5786/526/DC1
Materials and Methods
SOM Text
Figs. S1 to S10
References

18 April 2006; accepted 15 June 2006
10.1126/science.1128877

Multiple Phosphorylation Sites Confer Reproducibility of the Rod's Single-Photon Responses

Thuy Doan,[1] Ana Mendez,[4] Peter B. Detwiler,[2] Jeannie Chen,[4]* Fred Rieke[2,3]*

Although signals controlled by single molecules are expected to be inherently variable, rod photoreceptors generate reproducible responses to single absorbed photons. We show that this unexpected reproducibility—the consistency of amplitude and duration of rhodopsin activity—varies in a graded and systematic manner with the number but not the identity of phosphorylation sites on rhodopsin's C terminus. These results indicate that each phosphorylation site provides an independent step in rhodopsin deactivation and that collectively these steps tightly control rhodopsin's active lifetime. Other G protein cascades may exploit a similar mechanism to encode accurately the timing and number of receptor activation.

Rhodopsin may be biology's most precise single-molecule timekeeper. In retinal rod photoreceptors, the effective absorption of a single photon activates a single rhodopsin molecule, which triggers a highly amplified signal transduction cascade to produce a macroscopic change in the current flowing into the outer segment of the receptor. The electrical response evoked by a single photon shows much less trial-to-trial variability than other familiar signals generated by single molecules, such as the time to decay of a radioactive particle or the charge flowing through an ion channel during a single opening (*1*–*5*). More generally, events controlled by a first-order process (Fig. 1, A and B) are inherently more variable than the responses to single photons. Previous studies indicate that the low variability in the rod's current responses arises from low variability in the lifetime of light-activated rhodopsin (*2*–*6*). This poses a challenging molecular design problem: How is the active lifetime of a single molecule regulated so tightly?

Past work argues, largely by excluding other explanations, that reproducibility is produced by the deactivation, or shutoff, of a single rhodopsin molecule through a series of steps or transitions (*2*–*6*). The essence of this multistep shutoff model is simple averaging: The integrated rhodopsin activity averaged over multiple stochastic steps varies less than the activity controlled by a single step. Rhodopsin activity could be timed by the occurrence of each step before terminating with completion of the final step (Fig. 1, C and D), or rhodopsin activity could decline after each step (Fig. 1, E and F). In either case, the coefficient of variation (CV = standard deviation/mean) for rhodopsin's integrated activity is $1/\sqrt{N}$ for N independent steps that each control an equal frac-

[1]Program in Neurobiology and Behavior, [2]Department of Physiology and Biophysics, [3]Howard Hughes Medical Institute, University of Washington, Seattle, WA 98195, USA. [4]Department of Ophthalmology and Cell and Neurobiology Keck School of Medicine, University of Southern California, Los Angeles, CA 90089, USA.

*To whom correspondence should be addressed. E-mail: rieke@u.washington.edu (F.R.); jeannie@usc.edu (J.C.)

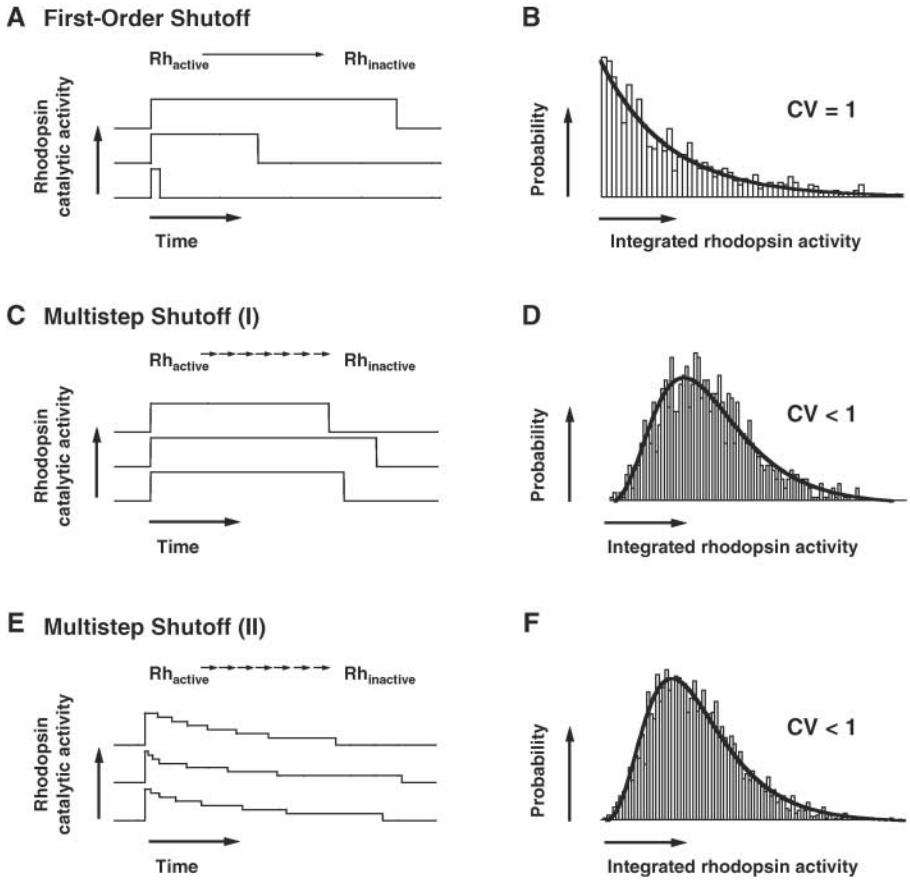

Fig. 1. Proposed models of rhodopsin shutoff. (**A**) Simulated activity of rhodopsin after a single stochastic shutoff step, (**C**) seven independent steps of equal rate constant where only the final step affects rhodopsin activity, and (**E**) seven independent steps where each step reduces an equal fraction of rhodopsin activity. (**B**, **D**, and **F**) Distributions of integrated rhodopsin activity from 1000 simulated responses, as in (A), (C), and (E). A first-order shutoff model predicts that the integrated rhodopsin activity is exponentially distributed with a $CV = 1$, whereas either multistep shutoff model predicts a $CV < 1$.

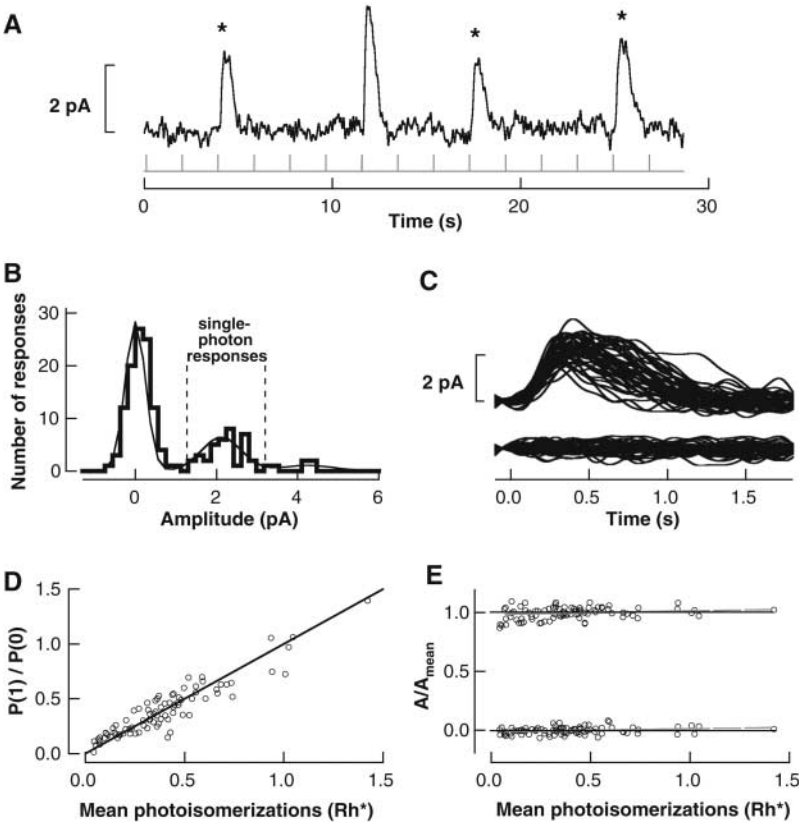

Fig. 2. Identification of single-photon responses in wild-type mouse rods. (**A**) Current responses recorded at 30°C to fixed-strength flashes (vertical bars) that produced on average 0.4 isomerizations. Asterisks indicate identified single-photon responses. Dark current = 17 pA; bandwith = 0 to 5 Hz. (**B**) Histogram of response amplitudes from the same rod and flash strength as (A). The fit (thin curve) was calculated using Eq. 1 [available in (*15*)]. Vertical dashed lines represent thresholds used to identify single-photon responses (*15*). (**C**) Graph of 50 consecutive single-photon responses and responses to zero absorbed photons isolated from the same rod as (A). (**D**) Average Rh* estimated from the ratio of the number of identified single-photon responses [$P(1)$] and responses to zero absorbed photons [$P(0)$] plotted against the average Rh* estimated from the collecting area and flash strength (29 cells). The points fall near the line of unity slope, indicating that the number of identified single-photon responses and responses to zero photons were consistent with expectations from Poisson statistics. Thus, systematic biases in the identification procedure were small. (**E**) Amplitudes of single-photon responses and responses to zero absorbed photons plotted against the strength of the flash (in Rh*) from which responses were identified. For each cell ($n = 29$), amplitudes (A) were normalized by the mean single-photon response amplitude (A_{mean}) for all flash strengths. Error-free identification predicts no dependence of the amplitude of the mean single-photon responses and responses to zero absorbed photons on flash strength (black lines). Slopes of the best-fit lines (dashed gray) through the data were 0.030 ± 0.003 (mean ± SD) for single-photon responses and 0.026 ± 0.002 for responses to zero absorbed photons, indicating that >90% of the single-photon responses were identified correctly. A similar low probability of errors in the identification of single-photon responses held for wild-type and transgenic rods.

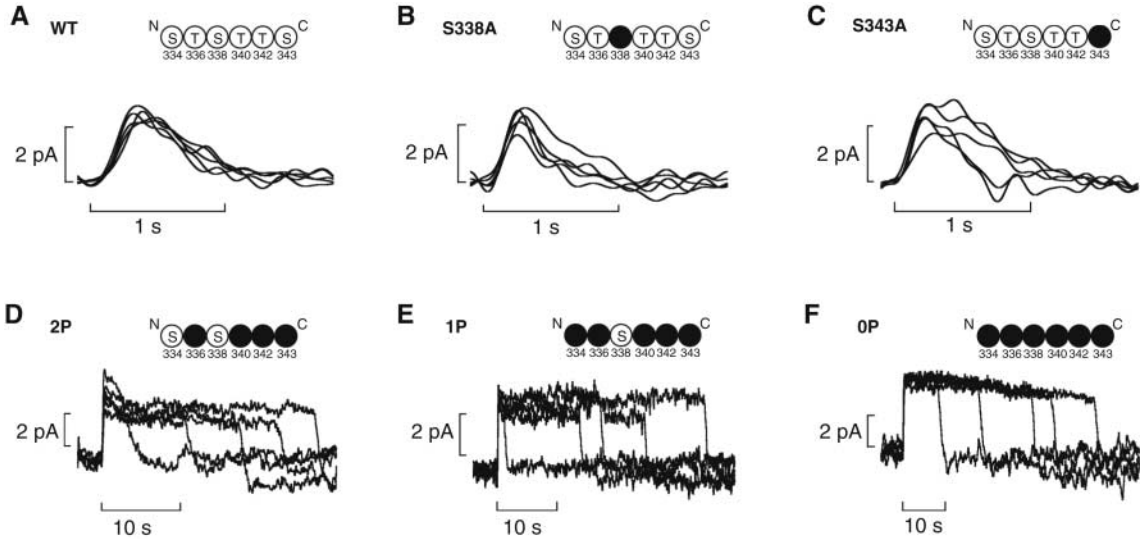

Fig. 3. Examples of single-photon responses produced by wild-type and mutated rhodopsin. Five identified single-photon responses from a mouse rod expressing (**A**) wild-type (WT) rhodopsin, (**B** and **C**) rhodopsin with five phosphorylation sites (S338A and S343A), (**D**) rhodopsin with two sites (2P), (**E**) rhodopsin with one site (1P), and (**F**) rhodopsin with zero sites (0P). Insets show simplified schematics of the C-terminal residues. Only the potential serine (S)/threonine (T) phosphorylation sites are shown. Black circles represent sites mutated to alanine. Response variability increases as the number of remaining phosphorylation sites decreases.

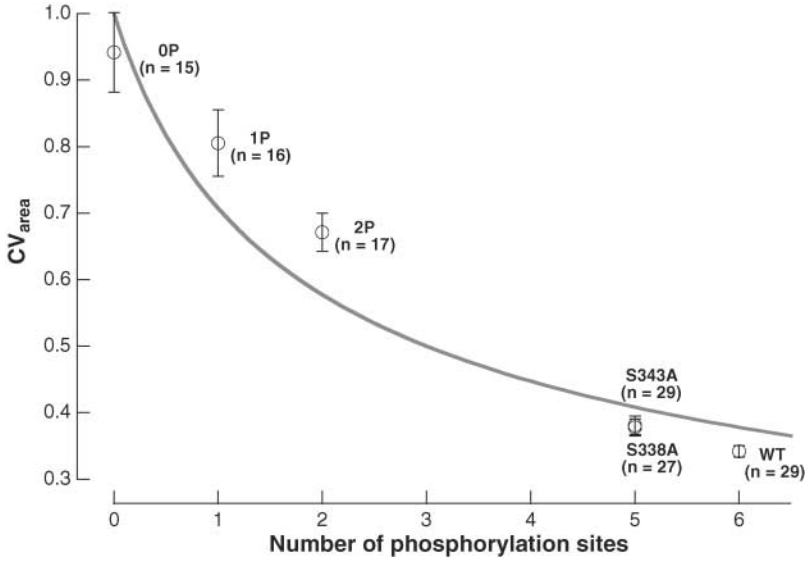

Fig. 4. Correlation of single-photon response variability with number of rhodopsin phosphorylation sites. Circles and vertical bars plot the mean CV_{area} ± SEM. The smooth curve is the CV_{area} predicted by $1/\sqrt{N_P + 1}$, where N_P is the number of phosphorylation sites and 1 represents arrestin binding.

tion of rhodopsin's integrated catalytic activity. Rhodopsin activity, similar to that of most G protein–coupled receptors, is terminated by phosphorylation and arrestin binding (*7*–*12*), leading to the proposal that multiple phosphorylations of rhodopsin provide the molecular steps for the multistep shutoff model (*4*, *13*, *14*). This hypothesis, however, has not been tested directly. The key missing element has been the ability to identify single-photon responses and quantify the effect of genetic manipulations on the activity of single rhodopsin molecules.

We characterized the variability of identified single-photon responses of wild-type and transgenic mouse rods to determine whether reproducibility depends on the number of rhodopsin phosphorylation sites in the graded and stochastic manner predicted by the multistep shutoff model. From single-cell recordings of the current flowing into the rod outer segment, we identified single-photon responses among responses to dim flashes producing on average 0.07 to 1.5 absorbed photons (Rh*) (*15*). These measured currents reflected the activity of light-activated rhodopsin molecules. Clear identification of single-photon responses requires the electrical current in response to the absorption of a photon to be distinguishable from the background current fluctuations and responses to multiple photons, requirements that were met in the recordings used here (Fig. 2, A and C) (*15*). Single-photon responses were separated from responses to zero and multiple absorbed photons by applying thresholds to histograms of the amplitude of the responses to a repeated dim flash (Fig. 2B). Tests for errors in identification (Fig. 2, D and E) indicated that <10% of the true single-photon responses failed to be identified and <10% of the identified responses were to zero or multiple absorbed photons (*5*, *15*).

We used the *CV* of the response areas (CV_{area}, the time integral of the response) to characterize the variability of the identified single-photon responses. The CV_{area} captures the total variability of the response, independent of whether the variability occurs early or late (fig. S1) (*5*, *14*). In the absence of saturation within the transduction cascade, the CV_{area} provides an upper bound on the variability of rhodopsin activity because components downstream of rhodopsin could also contribute. The CV_{area} for wild-type single-photon responses was 0.34 ± 0.01 at 30°C (mean ± SEM, n = 29) and 0.36 ± 0.02 at 35°C (n = 27). We performed all subsequent experiments at 30°C because the identification of single-photon responses was cleaner. Errors in identification of single-photon responses did not substantially influence the measured variability (*15*).

The proposal that the steps in the multistep shutoff model are provided by phosphorylation predicts that the CV_{area} of the single-photon responses will increase as the number of phosphorylation sites decreases, scaling as $1/\sqrt{N}$ for N independent and equal steps. We tested this prediction by quantifying the variability of identified single-photon responses in mouse rods expressing rhodopsin mutants with five, two, one, and zero remaining phosphorylation sites; wild-type rhodopsin has six phosphorylation sites (*4*). The number of sites was reduced by mutating serine or threonine residues to alanine (Fig. 3, insets) (*4*). Qualitatively, variability increased as the number of steps decreased (Fig. 3). Quantitatively, the CV_{area} in each case was near the $1/\sqrt{N}$ prediction, assuming that arrestin binding provided a final step in quenching rhodopsin activity (Fig. 4) (*10*).

The multistep shutoff model further predicts that reducing the number of phosphorylation sites from six to five should produce an ~8% increase in CV_{area}, independent of which site is removed. To test this prediction, we characterized single-photon responses from two rhodopsin mutants [Ser^{338}→Ala^{338} (S338A) and Ser^{343}→Ala^{343} (S343A)] with five phosphorylation sites (*4*). The measured CV_{area} was 0.38 ± 0.01 for S338A (n = 27) and 0.38 ± 0.02 for S343A (n = 29); both were significantly greater than the CV_{area} of 0.34 ± 0.01 of wild-type rods ($P < 0.001$ for S338A and $P < 0.05$ for S343A, Student's t test). The increase in CV_{area} was ~10%, very close to that predicted from the multistep shutoff model. The similar increase in variability of the S338A and S343A single-photon responses indicates that these sites make equal contributions to regulating rhodopsin shutoff.

The long duration of the single-photon responses in the mutants with one and two remaining phosphorylation sites suggested that a single shutoff step limited the duration of rhodopsin activity. If that is correct, rhodopsin shutoff should effectively be a first-order process, with a CV_{area} of 1 and an exponential distribution of lifetimes (Fig. 1, A and B). Thus, we were surprised to find a $CV_{area} < 1$ in these mutants. Whereas the durations of the single-photon responses produced by rhodopsin with zero phosphorylation sites were exponentially distributed (fig. S2C), those produced by rhodopsin with one or two remaining sites were not (fig. S2, A and B; $P < 0.05$ for two sites; $P < 0.002$ for one site, χ^2 test). The nonexponential lifetime distribution and CV_{area} less than 1 indicate either that phosphorylation occurs slowly in these mutants, and hence rhodopsin shutoff is still effectively controlled by several steps, or that arrestin binding itself is less stochastic than expected from a first-order process (*16*).

Although phosphorylation and arrestin binding are common steps in the shutoff of G protein–coupled receptors, many questions remain about the molecular details of these events. Our results provide some constraints. First, arrestin binding apparently controls a small fraction of the integrated rhodopsin activity under normal conditions, requiring that arrestin rarely binds to rhodopsin until most or all phosphorylation events have been completed. Indeed, biochemical measurements indicate that the affinity of rhodopsin for arrestin binding to rhodopsin increases as the number of phosphorylations increases (*13*, *17*). Second, each phosphorylation site could make an equal contribution to the shutoff of rhodopsin in one of two ways: (i) Rhodopsin's catalytic activity remains constant until arrestin binds and the rate constants associated with each phosphorylation event are equal (Fig. 1C), or (ii) each phosphorylation event decreases rhodopsin's catalytic activity and slows subsequent phosphorylation events (Fig. 1E). Previous measurements support the latter model (*5*, *10*, *13*), although combinations of the two are also possible.

We found that variability of the single-photon responses depended on the number of phosphorylation sites in a systematic and graded manner, including an increase in variability when a single site was removed. This result differs from past work that found that variability remained constant or decreased when one or three phosphorylation sites were removed (*4*). These previous experiments, however, were based on indirect estimates of single-photon response variability and thus could have missed the subtle increase in variability associated with the removal of a few phosphorylation sites. Although our results show that multistep shutoff through phosphorylation and arrestin binding is the dominant factor limiting variability of the rod's single-photon responses, we cannot rule out smaller contributions from other mechanisms. Indeed, single-photon responses of primate rods vary 20 to 30% less than those of mouse rods despite identical numbers of phosphorylation sites, suggesting that other mechanisms such as local saturation of the transduction cascade may help reduce response variability (*5*, *18*).

Vision in starlight requires detecting and processing responses to individual photons. Under these conditions, reproducibility of the single-photon response permits rods to encode accurate information about the number and timing of photon absorptions. Other G protein cascades—e.g., those in pheromone receptors (*19*, *20*)—operate when few receptors are active. Thus, receptor shutoff through multiple steps may be a general strategy to improve the fidelity of signals generated by G protein cascades.

References and Notes

1. D. Baylor, T. Lamb, K. Yau, *J. Physiol.* **288**, 613 (1979).
2. F. Rieke, D. Baylor, *Biophys. J.* **75**, 1836 (1998).
3. G. Whitlock, T. Lamb, *Neuron* **23**, 337 (1999).
4. A. Mendez *et al.*, *Neuron* **28**, 153 (2000).
5. G. Field, F. Rieke, *Neuron* **35**, 733 (2002).
6. M. Burns, A. Mendez, J. Chen, D. Baylor, *Neuron* **36**, 81 (2002).
7. U. Wilden, H. Kuhn, *Biochemistry* **21**, 3014 (1982).
8. H. Kuhn, S. Hall, U. Wilden, *FEBS Lett.* **176**, 473 (1984).
9. J. Chen, C. Makino, N. Peachey, D. Baylor, M. Simon, *Science* **267**, 374 (1995).
10. J. Xu *et al.*, *Nature* **389**, 505 (1997).
11. C. Chen *et al.*, *Proc. Natl. Acad. Sci. U.S.A.* **96**, 3718 (1999).
12. M. Kennedy *et al.*, *Neuron* **31**, 87 (2001).
13. S. Gibson, J. Parkes, P. Liebman, *Biochemistry* **39**, 5738 (2000).
14. R. Hamer, S. Nicholas, D. Tranchina, P. Liebman, T. Lamb, *J. Gen. Physiol.* **122**, 419 (2003).
15. Materials and methods are available as supporting material on *Science* Online.
16. V. Gurevich, E. Gurevich, *Trends Pharmacol. Sci.* **25**, 105 (2004).
17. U. Wilden, *Biochemistry* **34**, 1446 (1995).
18. S. Ramanathan, P. Detwiler, A. Sengupta, B. Shraiman, *Biophys. J.* **88**, 3063 (2005).
19. T. Leinders-Zufall *et al.*, *Nature* **405**, 792 (2000).
20. F. Zufall, K. Kelliher, T. Leinders-Zufall, *Microsc. Res. Tech.* **58**, 251 (2002).
21. We thank B. Hille, G. Murphy, F. Dunn, C. Asbury, B. Pinsky, J. Jensen, B. Wark, and A. Hinterwirth for constructive comments on the manuscript. Support was provided by the NIH through grants EY-11850 (F.R.), EY-12155 (J.C.), EY-02048 (P.B.D.), and T32EY-07031 (T.D.); Poncin Scholarship (T.D.); and the Howard Hughes Medical Institute (F.R.).

Supporting Online Material

www.sciencemag.org/cgi/content/full/313/5786/530/DC1
Materials and Methods
Figs. S1 and S2
References

23 February 2006; accepted 6 June 2006
10.1126/science.1126612

Activated Signal Transduction Kinases Frequently Occupy Target Genes

Dmitry K. Pokholok,[1]* Julia Zeitlinger,[1]* Nancy M. Hannett,[1] David B. Reynolds,[1] Richard A. Young[1,2]†

Cellular signal transduction pathways modify gene expression programs in response to changes in the environment, but the mechanisms by which these pathways regulate populations of genes under their control are not entirely understood. We present evidence that most mitogen-activated protein kinases and protein kinase A subunits become physically associated with the genes that they regulate in the yeast (*Saccharomyces cerevisiae*) genome. The ability to detect this interaction of signaling kinases with target genes can be used to more precisely and comprehensively map the regulatory circuitry that eukaryotic cells use to respond to their environment.

Signal transduction pathways mediate the cellular response to specific environmental or developmental signals. The activation of signal transduction pathways can lead to phosphorylation of transcription factors (*1*, *2*), histones (*3*), chromatin-modifying complexes, and the transcription machinery (*4*, *5*). These modifications contribute to changes in the gene expression program. Although the traditional view has been that most phosphorylation events do not occur at the genes that are ultimately controlled by signal transduction pathways, recent reports have revealed that at least one mitogen-activated protein kinase (MAPK)—high-osmolarity glycerol 1p (Hog1p) in yeast and its homolog p38 in

[1]Whitehead Institute for Biomedical Research, Nine Cambridge Center, Cambridge, MA 02142, USA. [2]Department of Biology, Massachusetts Institute of Technology, Cambridge, MA 02139, USA.

*These authors contributed equally to this work.
†To whom correspondence should be addressed. E-mail: young@wi.mit.edu